

Chapter 4

Bose-Einstein Condensation in a Dilute Gas: Measurement of Energy and Ground-State Occupation

4.1 Introduction

The ability to create Bose-Einstein condensation (BEC) in magnetically trapped alkali gases [22, 119, 142, 122] provided an opportunity to experimentally study the thermodynamics of bosonic systems in which the interactions are (i) weak, (ii) binary and (iii) experimentally adjustable [8, 121, 6]. One goal of experimental and theoretical work in this field was to understand a variety of low-temperature phenomena from both macroscopic and microscopic points-of-view, with a quantitative reconciliation of these two approaches. The experimental studies of collective excitations of zero-temperature condensates ([8, 143] and Chap. 3). were a step in this direction. The purpose of the present chapter is to explore the nature of the BEC phase transition by performing quantitative measurements of BEC in a different regime – near the critical temperature [144].

In this chapter we analyze a series of images of ultra-cold clouds of rubidium gas to determine the critical temperature and to extract ground-state occupation and total energy as a function of temperature. Total energy (or its derivative, specific heat) has a certain historical significance because it

was Fritz London's comparison [38] of the specific heats of liquid helium and an ideal Bose gas that began the rehabilitation of BEC as a useful physical concept. Moreover, measurements of thermodynamic quantities such as specific heat are essential in studying any phase transition. Ground-state occupation and critical temperature of a Bose gas are interesting because in liquid helium the former is very difficult to measure, while the latter is almost impossible to calculate accurately.

4.2 Experiment

The apparatus and procedures for creating BEC were the same as used in Sections 2.3 and 3.2. The imaging procedure used here differs in two specific ways. First, the atoms were always allowed to expand freely for a time of 10 ms before probing by the resonant probe beam. Secondly, we applied point-by-point corrections for imperfect polarization and saturation effects in our digital analysis to render the true 2-d projection of the velocity distribution in the expanded cloud.

4.3 Data Analysis

These distributions contain a wealth of thermodynamic information. For instance, the integrated area under the distribution is proportional to the total number, N , of atoms in the sample. The condensate appears as a narrow feature centered on zero velocity [22]; the number of atoms in the ground state, N_0 , is then proportional to the integrated area under this feature. From the mean square radius of the expanded cloud and the expansion time, we get the mean square velocity, or average energy, of the cloud. Finally, as discussed

below, the temperature, T , is extracted from the images, even though the temperature is not merely proportional to mean energy in a degenerate Bose cloud.

We went to some lengths to extract these thermodynamic quantities in a model-independent way. For instance, if we were to fit the observed velocity distributions to a Bose-Einstein distribution, we could hardly avoid coming to the conclusion that the specific heat is discontinuous - the singular behavior is built-in to the assumed functional form. Moreover, such a fit would preclude our being able to observe effects due to interactions, finite N , critical fluctuations, etc. Fortunately, useful thermodynamic information about the sample can be extracted from direct calculation of various moments of the velocity distribution, without specific reference to the nature of the distribution. The total number and energy of the atoms, as mentioned above, are simply proportional to the zeroth and second moments, respectively, calculated directly by summing over the velocity distribution images [145].

We defined the number of atoms in the ground state to be the number of atoms contributing to the narrow, central feature in the optical depth images [22]. To avoid biased and noisy results we provided the least-squares fitting routine with a tightly constrained template to use in its search for a condensate. With an independent set of measurements on condensates near zero temperature, we found that the condensate shapes were well-fit with 2-d Gaussians whose widths, aspect ratios and peak-heights, for a given trap frequency and expansion time, were functions only of the total number of atoms in the feature [6, 7]. The width, for instance, was parameterized by $\sigma = \sigma_o(1 + \alpha N_o)^{1/5}$, where σ_o is the predicted non-interacting condensate width and α was extracted empirically. The procedure yielded robust values of N_o , as long as the temper-

ature was high enough that the non-condensate atoms formed a distribution that was significantly broader than the sharp condensate feature. At temperatures below $T/T_o = 0.5$, both T and N_o measurements became suspect as it was no longer possible to cleanly separate the condensate and the non-condensate components without recourse to a detailed model, which was contrary to the spirit of this treatment.

Our thermometry differed from previously reported methods for ultracold trapped gases [22, 119, 142, 8, 121, 6, 143]. For an ideal gas far from quantum degeneracy the velocity distribution is a Gaussian whose width is proportional to $T^{1/2}$. As the cloud is cooled closer to the BEC phase transition, higher densities and lower temperatures cause a rapid increase in the significance of quantum statistics and of residual atom-atom interactions. Rather than attempt to model these effects, we assumed that the high-energy tail of the velocity distribution (i) remained in thermal equilibrium with the rest of the cloud and (ii) was characterized by a purely ideal Maxwell-Boltzmann (MB) distribution. The latter is plausible because these highest energy atoms spend most of their trajectories in the low-density, and therefore weakly interacting, outer part of the trapped cloud. Furthermore, the occupation numbers of the corresponding energy states are much less than one. Finally, during the free expansion, the high-energy atoms underwent on average much less than one collision. Guided by these assumptions, we determined the temperature by fitting a 2-d Gaussian to only the wings of our velocity-distribution images, excluding the central part of the cloud, where degeneracy, interactions, fluctuations, etc. may be significant. To test the assumption of thermal equilibrium we checked that the measured temperature of clouds were independent of the size of the exclusion region, outside of the degenerate regime [146].

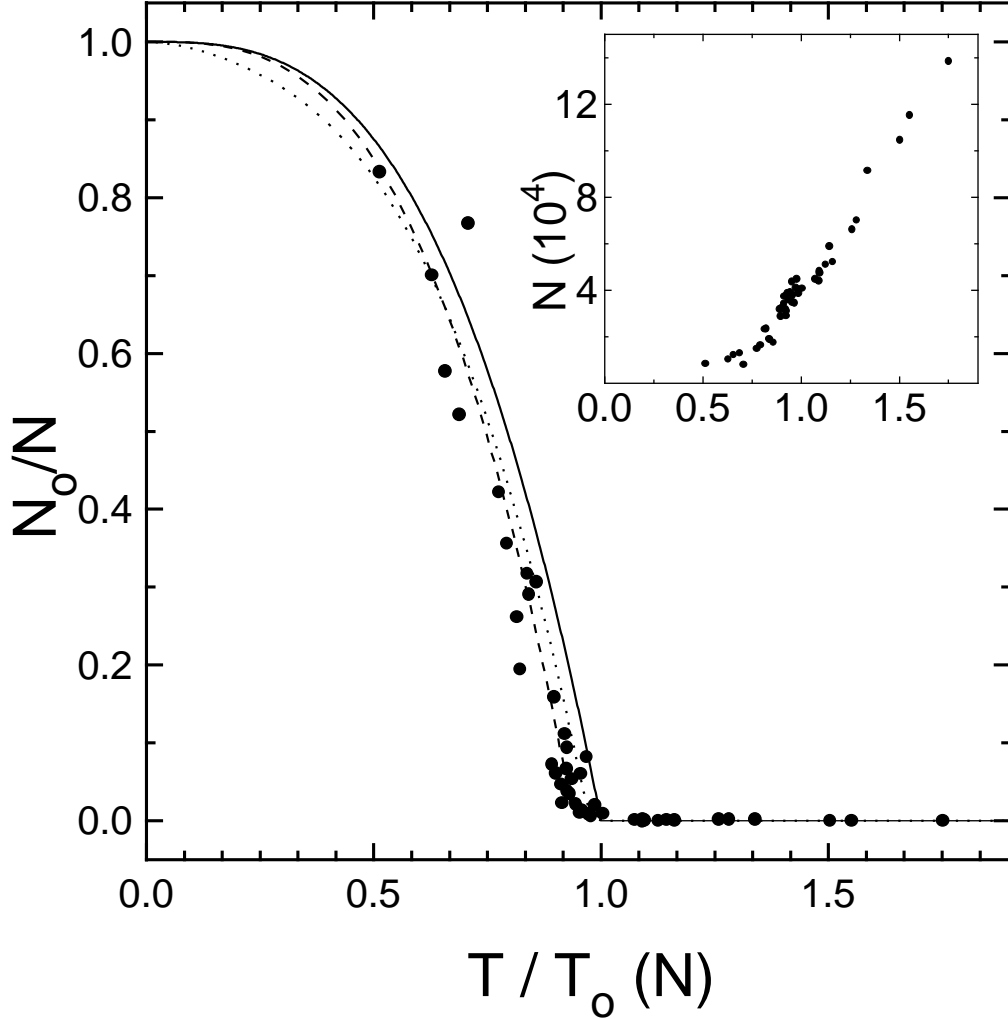


Figure 4.1: Total number N (inset) and ground-state fraction N_0/N as a function of scaled temperature T/T_0 . The scale temperature $T_0(N)$ is the predicted critical temperature, in the thermodynamic (infinite N) limit, for an ideal gas in a harmonic potential. The solid (dotted) line shows the infinite (finite) N theory curves. At the transition, the cloud consisted of 40,000 atoms at 280 nK. The dashed line is a least-squares fit to the form $N_0/N = 1 - (T/T_c)^3$ which gives $T_c = 0.94(5)T_0$. Each point represents the average of three separate images. Figure taken from Ref.[13].

4.4 Ground-State Fraction

The first quantity we examined is the ground-state fraction, N_o/N , as a function of scaled temperature T/T_o (Fig. 4.1). The temperature scaling removed the trivial shift in the transition temperature which occurred because as we evaporatively cool through the transition we also reduced the total number of atoms, N (Fig. 4.1, inset). We chose our scaling temperature to be $T_o(N) = \hbar\bar{\omega}/k_B(N/\zeta(3))^{1/3}$ where $\bar{\omega}$ is the geometric mean of the trap frequencies and ζ is the Riemann Zeta function. $T_o(N)$ is also the critical temperature, in the thermodynamic limit, for non-interacting bosons in a harmonic potential [147, 84]. For this case the temperature dependence of the ground-state fraction is $N_o/N = 1 - (T/T_o)^3$ below T_o (solid line, Fig. 4.1). We emphasize that, in contrast with the recent work of Mewes *et al.* [121], this line contains no free parameters and was not fit to the data, and so comparing this line to our data provides a detailed test of theory.

From our data we found a critical temperature of $T_c = 0.94(5)T_o$. The uncertainty was dominated by the systematic uncertainty in our measurement of the scaled temperature stemming mostly from a 2% uncertainty in the magnification of our imaging system. Our measurements were thus only marginally different from the theory for non-interacting bosons in the thermodynamic limit. Finite-number corrections [14, 15] will shift the transition temperature $T_c(N)$ down about 3% (dotted line, Fig. 4.1). Mean-field [84, 148] and many-body [149] interaction effects may also shift $T_c(N)$ a few percent.

4.5 Energy

The second result we present is a measurement of the energy and specific heat. Ballistic expansion, which facilitates quantitative imaging, also provided a way to measure the energy of a Bose gas [121, 6, 8]. The total energy per particle of the trapped cloud consists of harmonic potential, kinetic, and interaction potential energy contributions, or E_{pot} , E_{kin} and E_{int} , respectively. As the trapping field was non-adiabatically turned-off to initiate the expansion, E_{pot} suddenly vanished. During the ensuing expansion, the remaining components of the energy, E_{kin} and E_{int} , were then transformed into purely kinetic energy, E , of the expanding cloud: $E_{kin} + E_{int} \rightarrow E$, where E is the quantity we actually measured. According to the virial theorem, if the particles are ideal ($E_{int} = 0$), E will equal half the total energy, i.e. $E = 1/2 E_{tot}^{ideal}$. However, for a system with interparticle interactions the energy per particle due to E_{int} can be non-negligible and then $E = \alpha E_{tot}$, where α is not necessarily 1/2.

The scaled energy per particle, $E/Nk_B T_o$, is plotted versus the scaled temperature, T/T_o , in Fig. 4.2. E/N was normalized by the characteristic energy of the transition $k_B T_o(N)$ just as the temperature was normalized by T_o . The data shown were extracted from the same cloud images as those analyzed for the ground-state fraction. Above T_o , the data tended to the straight solid line which corresponded to the classical MB limit for the kinetic energy. Most interesting was the behavior of the gas at the transition. By examining the deviation, Δ , of the data from the classical line we saw (Fig. 4.2, inset) that the energy curve clearly changed slope near the empirical transition temperature ($0.94T_o$) obtained from the ground-state fraction analysis discussed above.

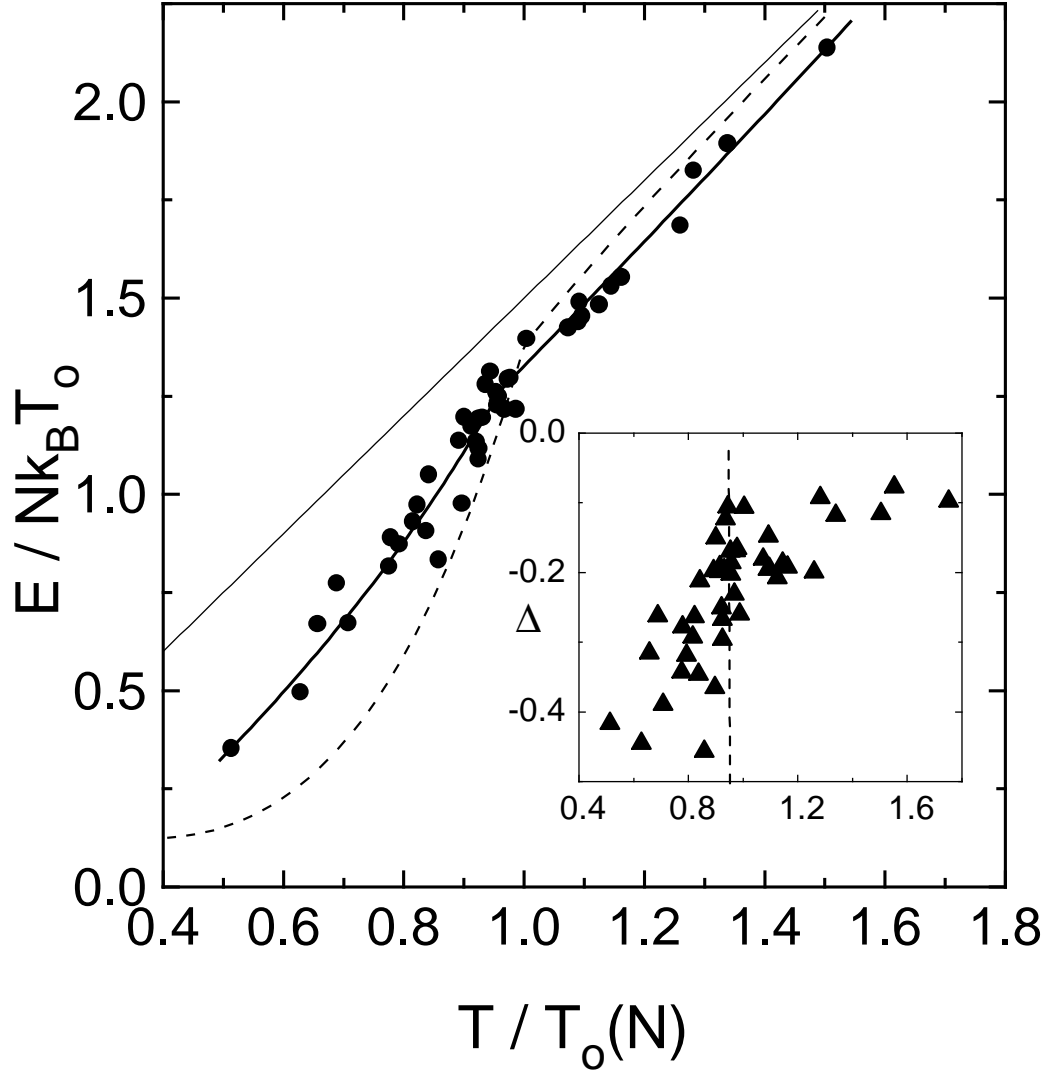


Figure 4.2: The scaled energy per particle $E/Nk_B T_0$ of the Bose gas is plotted vs. scaled temperature T/T_0 . The straight, solid line is the energy for a classical, ideal gas, and the dashed line is the predicted energy for a finite number of non-interacting bosons [14, 15]. The solid, curved lines are separate polynomial fits to the data above and below the empirical transition temperature of $0.94T_0$. (inset) The difference Δ between the data and the classical energy emphasizes the change in slope of the measured energy-temperature curve near $0.94T_0$ (vertical dashed line). Figure taken from Ref.[13].

4.6 Specific Heat

The specific heat is usually defined as the temperature derivative of the energy per particle, taken with either pressure or volume held constant. In our case the derivative was the slope of the scaled energy vs. temperature plot (Fig. 4.2), with neither pressure nor volume, but rather confining potential held constant. To place our measurement in context, it is instructive to look at the expected behavior of related specific heat versus temperature plots (Fig. 4.3). The specific heat of an ideal classical gas (MB statistics), displayed as a dashed line, is independent of temperature all the way to zero temperature. Ideal bosons confined in a 3-d box have a cusp in their specific heat at the critical temperature (dotted line) [38]. Liquid ^4He can be modeled as bosons in a 3-d box, but the true behavior is quite different from an ideal gas, as illustrated by the specific heat data [16, 17] (dot-dash line): the critical (or lambda) temperature is too low, and the gentle ideal gas cusp is replaced by a logarithmic divergence. We compared our data with the calculated specific heat of ideal bosons in a 3-d anisotropic simple harmonic oscillator (SHO) potential [147] (solid line). Note that because we did not measure E_{pot} , we had to divide the SHO theory values by two to compare with our measured expansion energies. The specific heat of the ideal gas is discontinuous and finite at the transition.

In order to extract a specific heat from our noisy data, we assumed that, as predicted, there was a discontinuity in the slope at the empirically determined transition temperature and fit the data to separate polynomials on either side of T_c (curved, solid lines in Fig. 4.2). We extracted the specific heat curve shown in Fig. 4.3 (bold line in inset). The observed step in the specific

heat at the critical temperature was considerably smaller than predicted by a finite number, ideal gas theory [14, 15] (Fig. 4.3, inset, thin line). A more sensible comparison is to avoid taking the model-dependent derivative and instead to compare theory and experiment directly in the energy-temperature plot (Fig. 4.2). The major deviation between the data and the SHO ideal gas theory (dotted line) occurs at scaled temperatures of 0.85 and below. The difference is probably due in part to the effects of interactions. Mean-field repulsion will tend to increase the energy at a given temperature.

4.7 Summary and Epilogue

We measured the critical temperature, ground-state occupation and energy of a dilute Bose gas of ^{87}Rb atoms. Our analysis was unique in that it did not rely on detailed models of the quantum degenerate cloud shape. We were thus able to examine the thermodynamics of the Bose gas in an unbiased and quantitative way. The measured ground-state fraction and transition temperature agreed well with the theory for non-interacting bosons. However, the qualitative features of the energy data are significantly different from the non-interacting theory.

Recent theoretical results [18, 150, 151] that consider the effects of mean-field interactions at finite temperature are in good agreement with our data. The theories adapt the standard Gross-Pitaevskii treatment [129, 5] to include the condensed and non-condensed components of the gas. Generally, mean-field interactions reduce the ground-state occupation and increase the energy per particle compared to the non-interacting Bose gas (in the thermodynamic limit) at the same temperature. A downward shift in the critical

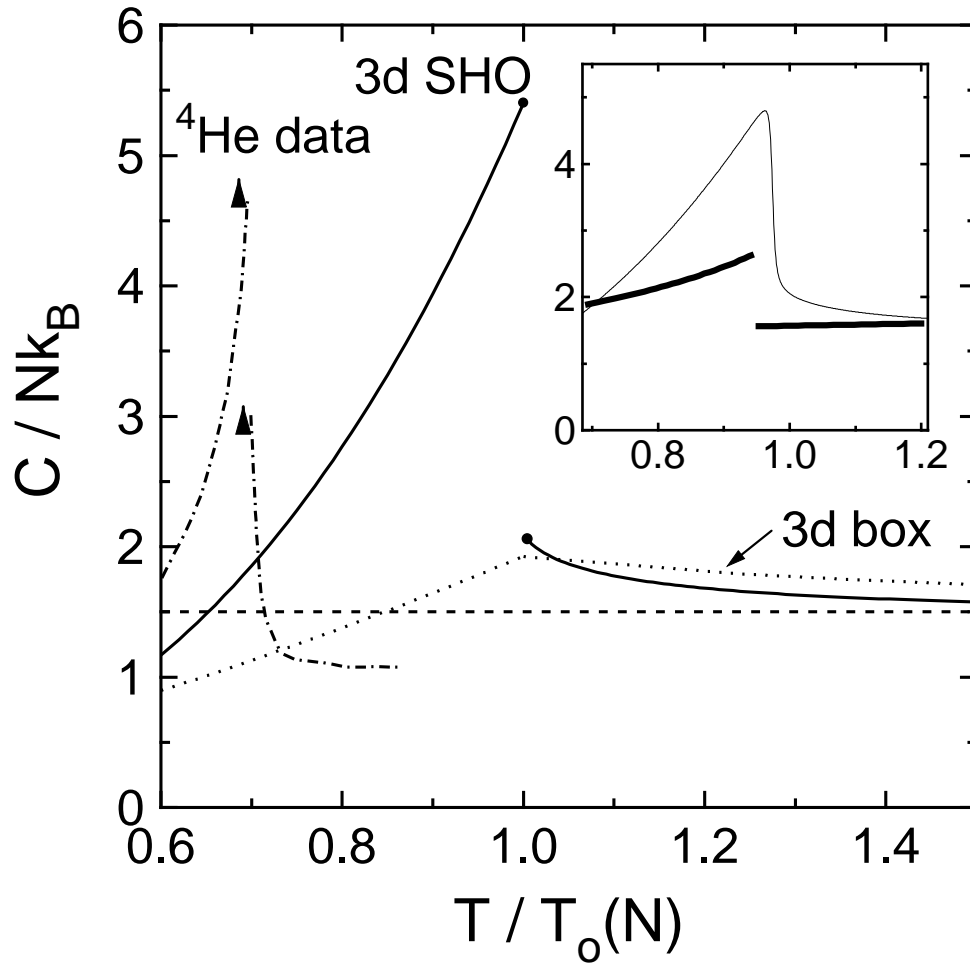


Figure 4.3: Specific heat, at constant external potential, vs. scaled temperature T/T_0 is plotted for various theories and experiment: theoretical curves for bosons in a anisotropic 3-d harmonic oscillator and a 3-d square well potential, and the data curve for liquid ^4He [16, 17]. The flat dashed line is the specific heat for a classical ideal gas. (inset) The derivative (bold line) of the polynomial fits to our energy data is compared to the predicted specific heat (fine line) for a finite number of ideal bosons in a harmonic potential. Figure taken from Ref.[13].

temperature due to finite number and mean-field is also predicted. Our data for the ground-state occupation lie between the mean-field predictions and the ideal gas model [18, 151]. Due to systematic uncertainties in our temperature measurement, the differences between our measurements and the recent theory are marginal, however. The predicted energy per particle is in excellent agreement with our measurements (Figure 4.4), including the observation of a feature in the specific heat.

In future work we will attempt to elucidate the role interactions play in the phase transition and the specific heat. For example, we can control the interactions by adjusting the magnetic trap spring constants and changing the number of trapped atoms [8]. In addition, with larger clouds [122] we can reduce our uncertainty in T_c , allowing us to investigate finite-number and mean-field effects at the 1% level.

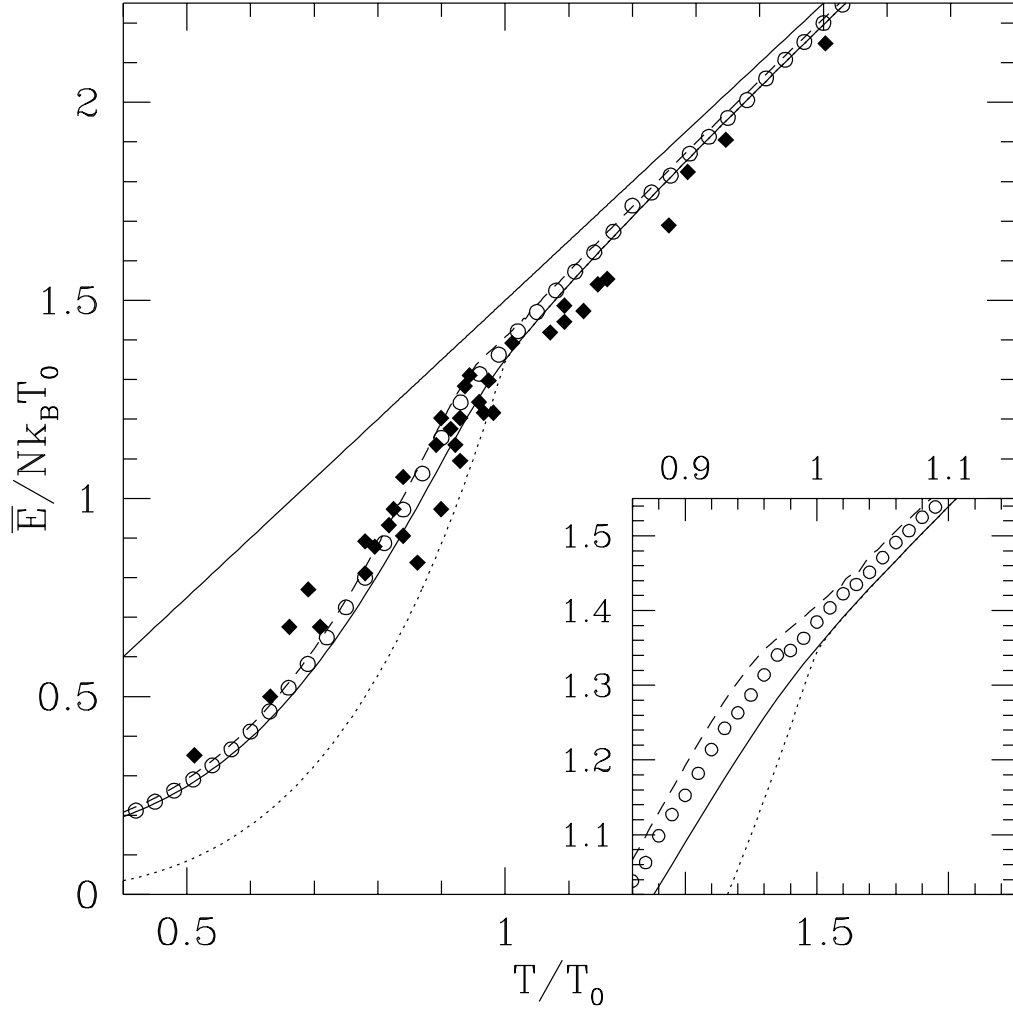


Figure 4.4: The sum of kinetic and interaction energy, as defined in the [18], obtained in the two-fluid model, compared with the data of Ensher *et al* [13] (diamonds) and with the ideal gas result (dotted curve). Results obtained from the zero-order solution (full curve), from the first-order perturbative treatment (dashed curve) and from the complete numerical solution (circles). The straight line is the classical Maxwell-Boltzmann result. The inset is an enlargement of the region around T_c . Figure taken from Ref.[18] with permission of S. Conti.